



Trade Science Inc.

ISSN : 0974 - 7486

Volume 7 Issue 1

Materials Science

An Indian Journal

Full Paper

MSAIJ, 7(1), 2011 [49-54]

Doped hydroxyapatite from waste calcium source: Part 2-Fe doped apatite

Samina Ahmed^{1*}, Mainul Ahsan¹, Sumaya F.Kabir², Ahmad I.Mustafa²

¹Institute of Glass and Ceramic Research and Testing (IGCRT),

Bangladesh Council of Scientific and Industrial Research (BCSIR), Dhaka-1205, (BANGLADESH)

²Department of Applied Chemistry and Chemical Engineering, University of Dhaka,
Dhaka-1000, (BANGLADESH)

E-mail : bcsir@yahoo.com

Received: 16th August, 2010 ; Accepted: 26th August, 2010

ABSTRACT

Doped hydroxyapatites with enhanced physical, chemical, mechanical and physiological stabilities have received significant attention as bone substitute materials, bone tissue engineering, orthopedics etc. Fe doped hydroxyapatite bio-ceramic material has been successfully synthesized from egg shell for the first time by wet chemical precipitation method. $(\text{NH}_4)_2\text{HPO}_4$ was used as the source of phosphate. Two different concentrations of doping solution were chosen to synthesize the doped apatite and the developed apatite was characterized by using FTIR, XRF, XRD and SEM techniques. Observed data were in excellent agreement with the standard values for hydroxyapatite which indicated that the change in concentration of doping solution did not affect the characteristics of the doped apatite.

© 2011 Trade Science Inc. - INDIA

KEYWORDS

Fe-doped apatite;
Hydroxyapatite;
Biocompatible;
Bone;
Cation.

INTRODUCTION

Hydroxyapatite (HA) being an analog material to bone and tooth mineral has been categorized as biocompatible, bioactive and osteoconductive (bone bonding ability with surrounding tissues)^[1-5]. However, wider applications of synthetic HA are somewhat restricted due to its *in-vivo* solubility and inferior mechanical properties which limits its use in load-bearing application^[1,6]. Thus, to get rid of these problems, attempts have been initiated by the researchers to synthesize doped HA. Since flexible structure of HA permits suitable cationic and anionic substitutions to enhance the mechanical and physiochemical stabilities,

doping treatment of HA has now become an important area of research^[7-10]. Hence, now-a-days researchers have put their best effort to develop modified synthetic apatites by the substitution or doping of chemical species found in natural bone. Such modification plays a significant role not only to produce HA with better mechanical and physiological stabilities but also to improve the suitability of HA for restoration of hard tissue such as bone and teeth^[2,9]. Moreover, incorporation of such species is also considered to have enormous effects on the mineralization, demineralization and re-mineralization processes occur in the calcified tissues^[11]. For instance, fluoride-substituted hydroxyapatite has better thermal and chemical stabilities than hydroxyapatite^[12].

Full Paper

However, vertebrate bone and tooth minerals is considered to contain HA structure with various substitution of Na^+ , K^+ , Fe^{3+} , Mg^{2+} , Sr^{2+} , Cl^- , F^- , HPO_4^- ions^[13,14].

Iron is one of the trace elements in bone and teeth^[13] and it is a vital element in the circulatory system, essential for the functioning of numerous proteins in cells^[14]. The presence of iron in HA lattice greatly influenced its solubility and crystallinity^[13]. Bio-compatible ferromagnetic ceramic materials exhibit promising characteristic for some bio-medical and therapeutic applications such as hyperthermia treatment for cancer and tumor masses, magnetic resonance imaging and release of drug^[15,16]. Hyperthermia treatment usually involves an external energy source, but the drawback of using such an external energy source is that it is also absorbed by the normal tissue while passing through the body. So, to overcome this limitation application of ferromagnetic bio-ceramics has now received significant attention. Such bio-ceramics upon implementation, around the tumor acts as thermo seeds and heat the tumor locally to 42°-46°C by their hysteresis loss when place under an alternating field^[15,16]. It is to be noted that, normal cells are not affected at this temperature. Thus, hydroxyapatite doped with iron oxide can be used for the treatment of bone cancer by hyperthermia and also can promote the bone formation^[15]. However, iron doped HA is super paramagnetic and also provides better biocompatibility than pure HA^[17].

Considering the diverse role of iron in biological functions, in this piece of work we have attempted to synthesize iron doped apatite by using waste egg shell as the prime raw material of Ca source. This would, undoubtedly be a cost-effective method and be also beneficial for creating an effective waste management technology. Moreover, such an effort will be a blessing mostly for those countries in which bio-ceramics have presently been imported.

EXPERIMENTAL

Materials

The chemicals FeCl_3 , NH_4OH , HNO_3 , $(\text{NH}_4)_2\text{HPO}_4$ used in this study were 99.99% pure analar grade, obtained either from E. Merck or BDH. All the solutions were prepared using double distilled water.

Synthesis of Fe doped HA

Prior to the synthesis of Fe doped apatite, the egg shells were cleaned, powdered and characterized as described in our previous approach^[18]. Iron doped HA was synthesized by following the earlier generalized wet chemical precipitation method^[18]. However, briefly requisite amount of egg shell powder was dissolved in conc. HNO_3 and the pH of the solution was changed to 10.0 with aqueous ammonia. At this stage first doping solution (0.1 M and 0.05 M FeCl_3) was mixed with the egg shell solution then ammonical $(\text{NH}_4)_2\text{HPO}_4$ (pH ~ 10.0) was added drop wise. The gelatinous precipitates of doped HA was kept for overnight and the precipitate was then filtered, washed and dried at 110°C to remove any trace of water. After oven drying calcinations was followed at 900°C. The calcined sample was then crushed to fine powder which was then subjected to characterization. To compare the results, pure HA (Ca/P=1.67) was also synthesized by following the above experimental procedure.

Characterization

Synthesized Fe doped HA was first analyzed to ensure the presence of Ca and P. Atomic absorption (AAS) and UV spectrophotometric methods were used to analyze these elements respectively. The presence of functional groups were determined by Fourier transform infrared spectroscopy (FT-IR, Model no. FT-IR-8900, SHIMADZU). Experimental spectra were obtained by using KBr disks with a 1:100 “samples-to-KBr” ratio and the samples were scanned in the wave number range of 4000 cm^{-1} -00 cm^{-1} with an average of 30 scans. The resolution of the spectrometer was 4 cm^{-1} . Phase purity of the prepared samples was investigated by using PANalytical (X'Pert PRO XRD PW 3040). The intensity data were collected in 0.02° steps following the scanning range of $2\theta = 20^\circ$ - 0° using $\text{CuK}\alpha$ ($\lambda = 1.54178^\circ\text{A}$) radiation. The observed phases were compared and confirmed using standard JCPDS files as described in the following section.

RESULTS

Figure 1 shows the typical FTIR spectrum of oven dried (110°C) iron substituted apatite, synthesized by using 0.1M doping while figure 2 presents the corre-

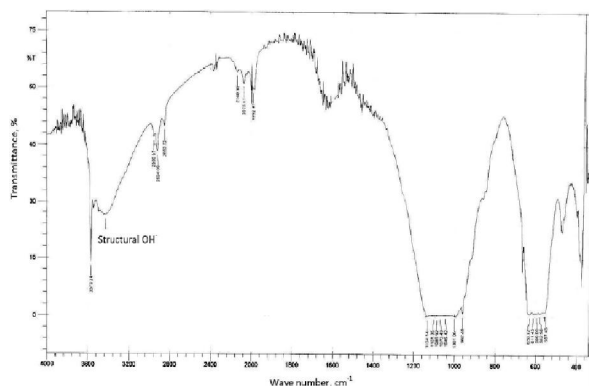


Figure 1 : Ftir spectrum oven dried of Fe_(0.1m)HA

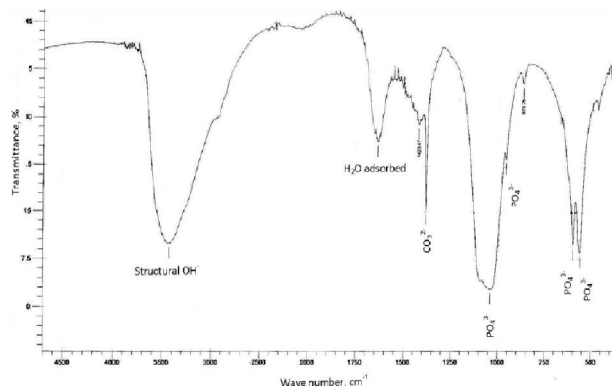


Figure 2 : Ftir spectrum of calcined Fe_(0.1m)HA

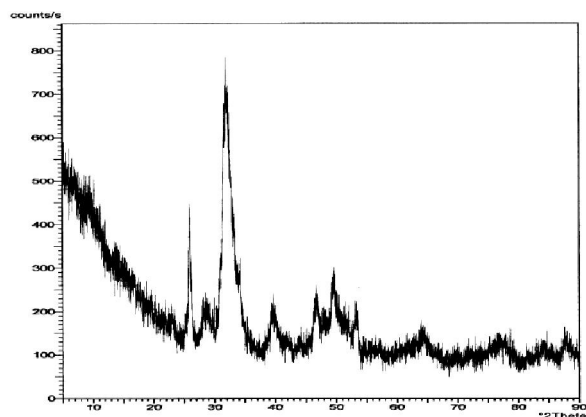


Figure 3 : Xrd spectra of oven dried Fe_(0.1m)HA

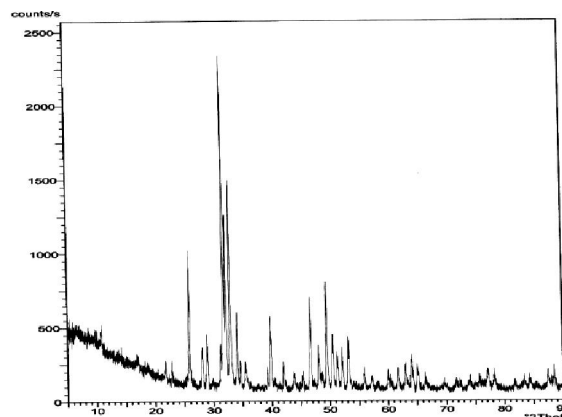


Figure 4 : Xrd spectra of calcined Fe_(0.1m)HA

sponding FTIR of calcined (900°C) Fe doped apatite. The recorded XRD patterns of the Fe-doped synthesized apatite (at 110°C and 900°C) are depicted in figure 3 and 4 respectively. SEM micrograph of the calcined (at 900°C) doped apatites (synthesized by using 0.1 M and 0.05 M doping solution) are shown in figure 5 and 6.

DISCUSSION

Characterization of Fe doped HA

Chemical analysis

The preliminary characteristic analysis i.e. the presence of Fe⁺³ ion in the substituted hydroxyapatites was confirmed by XRF analysis which also provided the Ca/P ratio as 1.66-1.67. This value is within the acceptable limit as found in pure HA.

FTIR analysis

The observed characteristic broad peaks (Figure 1) representing the phosphate (PO₄³⁻) group for the

oven dried samples supported the formation of apatite but in poor crystalline and amorphous nature. Additionally peaks for adsorbed water were also appeared in this case. This ill-defined crystalline behavior was dramatically changed to well crystalline form due to sintering at 900°C. The corresponding band positions representing the PO₄³⁻ group were evident as distinct, sharp peaks as expected (Figure 2). Particularly, the significant gap between the band positions of PO₄³⁻ group at 563.1 cm⁻¹ and 602.7 cm⁻¹ suggested the formation of well crystalline apatitic phase^[19]. This result was then subsequently confirmed from the XRD data which has been summarized in the next section. The presence of small peak for C-O vibration bonds of carbonate group at 1423 cm⁻¹ in Figure 2 provided the information that this sample contained carbonate ion and the presence of the carbonate ions promoted the incorporation of cation in the doped apatite^[11]. The visualized band positions and their corresponding assignments for 0.1 M and 0.05 M Fe doped apatites are tabulated in TABLE 1. Clearly the characteristic band positions observed

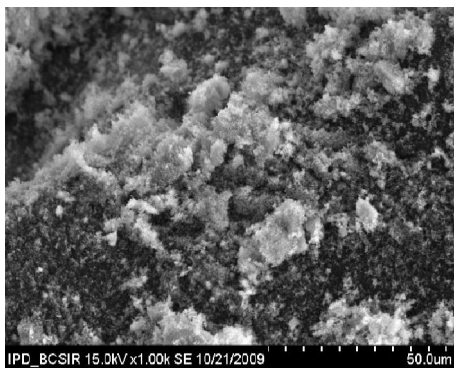


Figure 5 : Sem micrograph of calcined Fe_(0.1M) HA

for both of the synthesized samples are in good agreement with that of pure HA^[18,19]. This observation supported the formation of the expected cation substituted HA within the present experimental protocol.

XRD analysis

The broad peaks of the XRD spectrum (Figure 3) of the oven dried (at 110°C) Fe doped apatite shows a combination of the poorly crystalline and amorphous phase which supports the observed FTIR data. The reason of this nature is the temperature effect. It is well established that the degree of crystallinity increases with the increase of sintering temperature resulting several distinct peaks. Thus this low crystallinity and amorphous nature have been significantly changed to well-defined crystalline HA phase after heating the sample at 900°C (Figure 4). Clearly a number of prominent peaks for apatite phase were in the XRD diffraction pattern. However, the observed intensity and d-spacing values for both the samples (synthesized by using 0.1 M and 0.05 M doping solution) are in excellent agreement with the JCPDS standard data for HA^[19] as shown in TABLE 2. A brilliant matching of the strong diffraction peaks at 2θ positions $\sim 31.78^\circ$ (2 1 1) together with other two peaks at $\sim 32.26^\circ$ (1 1 2) and $\sim 32.95^\circ$ (3 0 0) ensured the formation of well crystallized doped apatite at 900°C. This observation confirmed the formation of Fe substituted apatite of hexagonal structure and strictly proved that a variety of substitutions of both cationic and anionic is possible in hydroxyapatite structure without any significant modification of its hexagonal system as mentioned in the previous investigation^[11].

The crystallite size, crystallinity and cell volume of both of the calcined (at 900°C) doped samples were calculated as described previously^[18]. The calculated

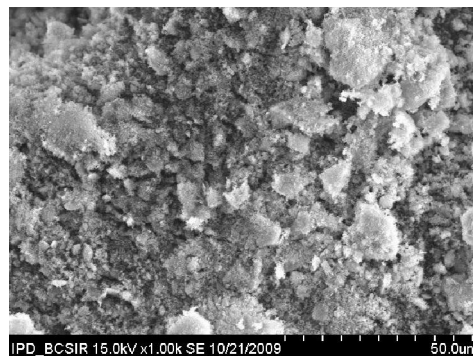


Figure 6 : Sem micrograph of calcined Fe_(0.05M) HA

values were tabulated in TABLE 3. The lattice parameters and cell volume values of the 0.05 M Fe-doped apatite did not significantly changed as compared to those values of pure HA^[18] but in case of 0.1 M doped apatite, lattice parameters and cell volume values are lower that observed in case of pure HA^[18]. However for both cases lower values of crystallite size and crystallinity were observed as substitution reduces significantly the crystallite size as well as crystallinity^[7]. Possibly, the changes in cell volume for the later case would be due to the substitution of more cation (since 0.1 M Fe doping solution was used in this case).

SEM analysis

As the crystallinity of apatites strictly depends on the sintering temperature and as a consequence it has already been shown that synthesized apatite usually forms in well crystalline shape only after sintering at 900°C, so the morphology and micro structural features of the crystalline Fe substituted apatites synthesized at this temperature were further examined by capturing their SEM micrographs. The recorded SEM pictures (Figure 5 and 6) for calcined (at 900°C) apatites appeared with having a combination of different regular but agglomerated shapes, such as hexagonal, spherical, etc.

CONCLUSION

Fe substituted or doped hydroxyapatite has been successfully synthesized from egg shell for the first time, which could be a potential and cost-effective bio-ceramic material for bone substitution in surgery, orthopedics and dentistry fields. The synthesized doped apatites were characterized by XRF, FTIR, XRD and SEM techniques and resembled the characteristics of

TABLE 1 : FTIR band positions and corresponding assignments of calcined pure and Fe cation doped apatites

Observed band positions (cm ⁻¹)			Corresponding assignments
Pure HA	Fe _(0.05) HA	Fe _(0.1) HA	
570.9	561.2	565.1	PO ₄ ³⁻ bending (ν ₄)
601.7	602.3	603.7	PO ₄ ³⁻ bending (ν ₄)
962.4	961.3	962.4	PO ₄ ³⁻ stretching(ν ₁)
1039.6	1016.2	1014.56	PO ₄ ³⁻ bending (ν ₃)
-----	1419.3	1423.47	CO ₃ ²⁻ group (ν ₃)
1650.0	1633.2	1639.4	H ₂ Oadsorbed(ν ₂)
3500.00	3231.52	3431.3	Structural OH ⁻

TABLE 2 : Relative intensity and d- spacing (hexagonal unit cell) for calcined pure ha and Fe doped HA

Fe _(0.1) HA		Fe _(0.05) HA		Pure HA	
d-spacing	relative intensity	d-spacing	relative intensity	d-spacing	relative intensity
4.0710	8.62	4.0787	9.28	4.0748	6.38
3.8682	6.93	3.864	9.36	3.8999	4.45
3.4332	52.03	3.4353	38.68	3.4395	38.68
3.1835	12.35	3.1649	12.33	3.1673	8.36
3.0824	12.31	3.0827	7.25	3.0861	14.60
2.8068	100	2.8119	100.00	2.8152	100.00
2.7735	61.11	2.774	52.90	2.7744	59.40
2.7180	59.53	2.7148	62.30	2.7183	55.42
2.6279	13.03	2.6298	20.99	2.6296	23.44
2.5238	27.23	2.5257	6.93	2.5271	5.30
2.2589	7.88	2.2604	22.47	2.2619	19.31
2.1450	24.11	2.1480	8.60	2.1482	5.28
2.0587	6.71	2.0594	5.27	2.0610	5.54
1.9417	5.10	1.9427	26.62	1.9443	28.19
1.8879	28.63	1.8891	13.43	1.8914	14.58
1.8414	15.17	1.8344	17.07	1.8413	32.19
1.8044	27.79	1.8042	15.39	1.8060	15.67
1.7789	17.08	1.7778	11.76	1.7806	11.83
1.7534	12.84	1.7538	12.50	1.7538	12.30

TABLE 3 : Crystallographic information of calcined Fe substituted apatites

Parameters	Calcined Fe _(0.05M) HA	Calcined Fe _(0.1M) HA	Calcined HA
Lattice parameter a=b	9.42	9.40	9.42
c	6.87	6.85	6.88
Crystallinity, x _c	4.37	3.54	5.03
Crystal size (°A)	525.39	467.09	752.37
Volume	1578.30	1567.70	1580.60

pure HA. The change in concentration of doping solution did not affect the formation of desired doped

apatite. However, incorporation of such cation in hydroxyapatite structure will play a vital role to enhance the bioactivity and physiochemical properties of the apatite. On the other hand utilization of egg shell will open up an effective trail for waste management through material re-cycling approach which will ultimately be a significant step towards a green and clean environment.

ACKNOWLEDGEMENT

We acknowledge the financial support from IGCRT, BCSIR and the assistance of Dr. Mohammad Mizanur Rahman, Assistant Professor of ACCE, DU for FTIR. We also appreciate the generosity of the Ministry of Science and Information & Communication Technology, Government of Bangladesh for granting the NSICT fellowship to SFK.

REFERENCES

- [1] T.J.Webster, E.A.Massa-Schlueter, J.L.Smith, E.B.Slamovich; *Biomaterials*, **25**, 2111-33 (2004).
- [2] F.Ren, R.Xin, X.Ge, Y.Leng; *Acta Biomaterialia*, **5(8)**, 3141-3149 (2009).
- [3] S.J.Kalita, H.A.Bhatt; *Materials Science and Engineering C*, **27**, 837-848 (2007).
- [4] M.E.Fleet, X.Liu; *Biomaterials*, **28**, 916-26 (2007).
- [5] F.Miyaji, Y.Kono, Y.Suyama; *Materials Research Bulletin*, **40**, 209-220 (2004).
- [6] Y.Li, C.Teck Nam, C.P.Ooi; *Journal of Physics: Conference Series*, **187**, 012-024 (2009).
- [7] K.K.Mallick; *Ceramic Processing Research*, **9(3)**, 7-13 (2008).
- [8] K.A.Gross, R.Jackson, J.D.Cashion, L.M.Rodriguez-Lorenzo; *European Cells and Materials*, **3(2)**, 114-117 (2002).
- [9] Y.Tang, H.F.Chappell, M.T.Dove, R.J.Reeder, Young J.Lee; *Biomaterials*, **30**, 2864-2872 (2009).
- [10] A.C.Tas, S.B.Bhaduri, S.Jalota; *Materials Science and Engineering C*, **27(3)**, 394-401 (2007).
- [11] S.Kannan, J.M.G.Ventura, A.F.Lemos, A.Barba, J.M.F.Ferreira; *Ceramics International*, **34**, 7-13 (2008).
- [12] H.Eslami, M.Solati-Hasjin, M.Tahriri; *J.of Ceramic Processing and Research*, **9(3)**, 224 (2008).
- [13] J.Wang T.Nonami, K.Yubata; *J.Mater.Sci: Mater.Med.*, **19**, 2663-2667 (2008).

Full Paper

- [14] K.Donadel, M.D.V.Felisberto, M.C.M.Laranjeira; An.Acad.Bras.Cienc., **81(2)**, 179-186 (**year**).
- [15] S.Deb, J.Giri, S.Dasgupta, D.Datta, D.Bahadur; Bull.Mater.Sci., **26(7)**, 655-660 (**2003**).
- [16] H.C.Wu, T.W.Wang, J.S.Sun, W.H.Wang, F.H.Lin; Nanotechnology, **18**, 165-601 (**2007**).
- [17] F.P.Filho, R.E.F.Q.Nogueira, M.P.F.Grac-a, M.A.Valente, A.S.B.Sombra, C.C.Silva; Physica B, **40(3)**, 3826-3829 (**2008**).
- [18] S.F Kabir, S.Ahmed, M.Ahsan. A.I.Mustafa; TSI submitted, (**2010**).
- [19] S.Ahmed, M.Ahsan; Bangladesh J.Sci.Ind.Res., **43(4)**, 501-512 (**2008**).